Journal of Applied Mechanics and Technical Physics, Vol. 50, No. 2, pp. 278–283, 2009

FORCE ACTION OF DISCONTINUOUS WAVES ON A VERTICAL WALL

V. I. Bukreev

UDC 532.532+532.59

This paper presents the results of an experimental study of the dynamic action exerted on the vertical end wall of a rectangular channel by the wave propagating in the tailwater region after total dam break. It is shown that the results of calculations using the first shallow-water approximation differ from experimental data by not more than 5%.

Key words: *moving hydraulic jump (bore), reflection from vertical wall, force action.*

Introduction. The dynamic action of waves on various obstacles and floating bodies has been a subject of extensive research, which has shown, in particular, that the shape of the incident wave is of considerable significance in this problem. Previous studies, however, have dealt primarily with sinusoidal, standing, solitary, and wind waves. The present paper considers the effect of the waves formed in the tailwater region after dam break (in shallow water theory and gas dynamics, the corresponding waves are called discontinuous [1, 2]). In the theoretical analysis of these problems, the term the discontinuity decay problem is used. In the present work, we consider the particular case of the discontinuity decay problem where the fluid is initially at rest.

The tailwater wave produced by dam break is referred to as the dam-break wave [3]. The dam-break wave is the simplest example of catastrophic waves of various natures. The kinematic characteristics of such waves (height, propagation speed, and the velocity of the wave-induced fluid motion) have been well studied both theoretically and experimentally. In the case of a parabolic (in particular, rectangular) channel, analytical solutions have been obtained using the first shallow-water approximation [1, 2]. In a real river bed with flood beds, lateral inflows, and various hydraulic resistances, the kinematic characteristics of dam-break waves are determined by numerical calculations using the Saint Venant equations [3, 4]. The corresponding calculations for small time intervals have also been performed using more complex mathematical models [5–8]. Among the great number of experimental studies, mention should be made of papers [9,10], which provided support for the analytical solutions used below [1, 2]. The dynamic action of dam-break waves on various obstacles has been the subject of a few studies, all of which were experimental [11–14].

The dynamic action on the wall blocking the cross-section of a channel can be calculated using the above-mentioned theories. The purpose of the present work was to experimentally verify the calculation results based on theoretical studies [1, 2]. The results of methodologically close experiments are given in [11, 12], but these papers consider a short channel with a nonhorizontal bottom and nonvertical end wall, which differs from the formulation of the problem in [1, 2].

The fluid velocity and depth and the pressure at the front of a theoretical discontinuous waves changes suddenly. Such a model wave has an instantaneous impact on the obstacle, after which the flow pattern becomes stationary. In practice, dam-break waves have the form of a moving hydraulic jump, whose length is, at least, five times its height [15]; therefore, the force acting on the obstacle reaches a constant value continuously.

A moving hydraulic jump is termed a bore [2, 3]. There are five types of hydraulic jump and bore [3, 15]; four types are characterized by the presence of undulations — nonlinear oscillations in the fluid depth and

Lavrent'ev Institute of Hydrodynamics, Siberian Division, Russian Academy of Sciences, Novosibirsk 630090; bukreev@hydro.nsc.ru. Translated from Prikladnaya Mekhanika i Tekhnicheskaya Fizika, Vol. 50, No. 2, pp. 129–135, March–April, 2009. Original article submitted October 29, 2007.

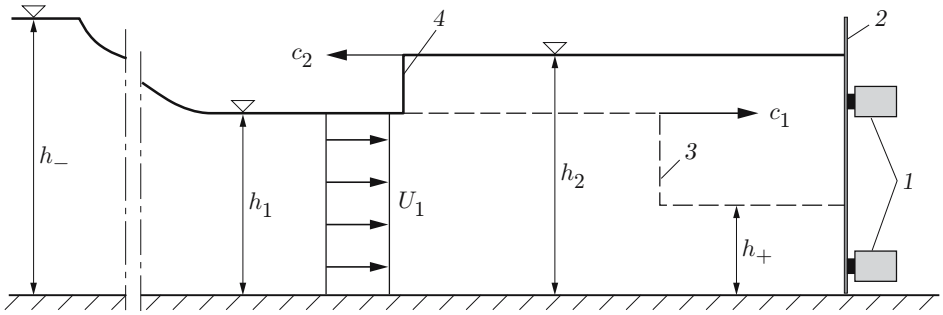

Fig. 1. Diagram of experiment: 1) force sensors; 2) plate (wall); 3) incident wave; 4) reflected wave.

velocity in some region behind the leading edge of the bore. Under some conditions, the undulation amplitude is comparable to the average height of the bore. Undulations are rapidly degenerated, which is due primarily to the effect of dispersion rather than viscosity. Upon the reflection from the vertical wall, the undulation amplitude increases [10]. If a dam-break wave impacts a plate or a cylinder that block the flow only partially, the presence of undulations leads to a considerable increase in the force and the overturning moment of the force relative to the channel bottom [13, 14].

1. Kinematic Characteristics of Incident and Reflected Waves. Figure 1 shows the theoretical profiles of the incident and reflected waves in the case of an initially flooded bottom in the tailwater ($h_+ > 0$). According to theoretical papers [1, 2], the incident-wave profile $h(x,t)$ is described by the relations

$$h = h_- \quad \text{at} \quad x < -c_0 t, \qquad h = (2c_0 - x/t)/(9g) \quad \text{at} \quad -c_0 t \leqslant x \leqslant (2c_0 - 3c_*)t,$$

$$h = h_1 \quad \text{at} \quad (2c_0 - 3c_*)t < x < c_1 t, \qquad h = h_+ \quad \text{at} \quad x \geqslant 2c_1 t,$$

where x is the longitudinal coordinate (at the shield location, $x = 0$, and in the tailwater, $x > 0$), t is time, g is the acceleration due to gravity, and h_- and h_+ are the initial headwater and tailwater depths. The parameters of this wave are found from the system

$$c_0 = \sqrt{gh_-}, \qquad (h_1 - h_+)\sqrt{g(h_1 + h_+)/(2h_1 h_+)} = 2(\sqrt{gh_-} - \sqrt{gh_1}),$$

$$c_* = \sqrt{gh_1}, \qquad c_1 = c_*\sqrt{(h_1 + h_+)/(2h_+)}, \qquad U_1 = c_1(1 - h_+/h_1).$$

In the analysis of the dynamic impact, the incident wave, which is a combination of a centered level-depression wave and a simple discontinuous wave, has the following important features. The depression wave becomes the discontinuous wave in the flow cross-section with the coordinate $x_* = c_* t$. For $c_* = 2c_0/3$, $x_* = 0$, which occurs at $h_+/h_- \simeq 0.138$. If $c_* < 2c_0/3$ $(h_+/h_- > 0.138)$, conjugation of the depression wave and the discontinuous waves occurs in the headwater, the point of conjugation is displaced upstream with time, and the tailwater flow is subcritical [$\mathrm{Fr} = U_1^2/(gh_1) < 1$]. This state of head and tail conjugation is called submerged. If $c_* > 2c_0/3$ $(h_+/h_- < 0.138)$, conjugation of the depression wave and discontinuous waves occurs in the tailwater, the point of conjugation is displaced downstream with time, and the tailwater flow is supercritical ($\mathrm{Fr} > 1$). This state of head and tail conjugation is called free.

In the case of the free state of head and tail conjugation, reflection from the wall results in an upstream propagating continuous wave (see Fig. 1) with the following parameters:

$$h_2 = h_1 + U_1\sqrt{2h_1 h_2/(g(h_1 + h_2))}, \qquad c_2 = -U_1 h_1/(h_2 - h_1).$$

Behind the reflected-wave front, the theoretical velocity $U_2 = 0$, and the force acting on the vertical end wall of the rectangular channel after the reflection of the theoretical wave is constant in time and is calculated by the formula

$$F_T = 0.5\rho g h_2 B,$$

where ρ is the fluid density and B is the channel width. In the case of the free state of head and tail conjugation, this formula is valid only before the time $t_* = l/c_*$ (l is the distance from the shield to the end wall of the channel; in the headwater region, the channel is considered infinitely long). After that, the depth h_2 and the force F_T increase. Figures 2–6 give only constant theoretical values of h_2 and F_T.

In the case of an initially dry bottom in the tailwater region ($h_+ = 0$), only the depression wave remains, whose profile is described by the above relations where $h_1 = h_+ = 0$ and $c_* = 0$. After reflection of this wave from the wall, the force increases continuously with time.

The validity of the condition of transition from the free state to the submerged state of head and tail conjugation and the validity of the formulas for h_1 and c_1 is confirmed by experiments [9, 10]. The results of an experimental verification of the formulas for h_2 and c_2 are given below. In the case of a dry bottom in the tailwater region, the profile and characteristic speeds of propagation of the wave are in poor agreement with experimental data [10].

In theoretical studies [1, 2], a hydrostatic pressure distribution ahead of and behind the discontinuous-wave front is assumed. In experiments, the initial stage of reflection involves water splash on the wall [16], which enhances the undulations. During the water splash and at the head of the experimental wave, the pressure distribution is not hydrostatic.

2. Experimental Technique and Analysis of Measurement Results. The experiments were performed in the rectangular channel with an even horizontal bottom that has been used in previous experiments [10] (channel width $B = 0.2$ m, length $L = 8.2$ m, and height 0.25 m). At a distance $l = 2$ m on the left of the end wall of the channel there was a thin flat vertical shield, which produced an initial difference in depth between the headwater and tailwater regions. A the time $t = 0$, the shield was rapidly (in approximately 0.04 sec) lifted upward.

The plate (see Fig. 1) was fixed on Honeywell rigid force sensors. Between the plate, the lateral walls, and the channel bottom there were gaps of size 3 mm covered with a thin rubber film. The small force acting on the rubber film was taken into account during calibration of the measuring system. Static calibration of the measuring system was performed directly during the experiments by stepwise changing the depth of the quiescent fluid with a strictly hydrostatic pressure distribution. Dynamic calibration was performed by a short-term impact on the plate in the quiescent fluid. The eigenfrequency ω_0 and damping decrement α of the measuring system were determined from the response of the system to the impact using a standard method. These parameters depended primarily on the mass of the plate and the added mass of water since the plate rested on the sensors with an eigenfrequency of about 10^5 sec^{-1}. For the most unfavorable measurement conditions, the values $\omega_0/(2\pi) = 8.3$ sec^{-1} and $\alpha = 14$ sec^{-1} were obtained. Next, it was shown that, at frequencies $\omega/(2\pi) \geqslant 2.5$ sec^{-1}, the spectra of the forces are nearly zero and, hence, frequency distortions during the measurements could be ignored.

Free-surface oscillations in time for several fixed values of the coordinate x on the channel axis were measured by wavemeters operating on the principle of a large difference in electrical conductivity between water and air. The 1-mm diameter sensing electrodes of the wavemeters were spaced 5 mm apart in the cross-sectional plane of the incident flow. Static calibration of the wavemeters was performed by stepwise lifting of their electrodes for a specified distance in the quiescent fluid. During dynamic calibration, the electrodes were moved sinusoidally at varied frequency. It was found that frequency distortions could also be ignored in wave measurements.

The electrodes of one of the wavemeters were placed at a distance of 10 mm upstream from the plate. The other two wavemeters were placed at different distances x from the shield in different series of experiments, so that the interval Δx between them was constant and equal to 0.3 m. The time $\Delta t_{1,2}$ required for the middle (in height) points of the leading edges of the direct and reflected waves to travel this distance were used to determine the quantities $c_{1,2} = \Delta x/\Delta t_{1,2}$, which were compared with theoretical propagation speeds of waves c_1 and c_2, respectively.

Primary information was analyzed with the aid of a computer. Repeated measurements were performed on different days under the same conditions. In each experiment, the standard deviation did not exceed 2% for measurements of the depth and force F and 3% for the wave-propagation speed. After averaging over four experiments and B-spline smoothing of the data for various initial depths, the error decreased. The spread of the experimental points is given in Figs. 4–6.

In [1, 2], wave propagation is determined only by the parameters $h_+^0 = h_+/h_-$ and g (see the formula given above). In experiments, it is necessary to take into account the fluid viscosity, the finite channel dimensions, and the roughness of the solid boundaries. In the present study, a comparison with theory was performed only for such time intervals for which the effect of these slow-acting factors did not exceed the measurement error. The parameter h_+^0 was varied in the range $0 \leqslant h_+^0 \leqslant 0.84$.

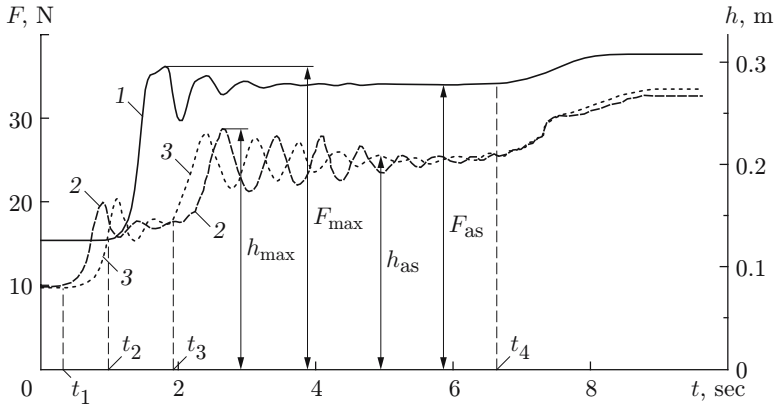

Fig. 2. Time evolution of the force (curve 1) and depth behind the incident-wave front (curve 2) and reflected-wave front (curve 3).

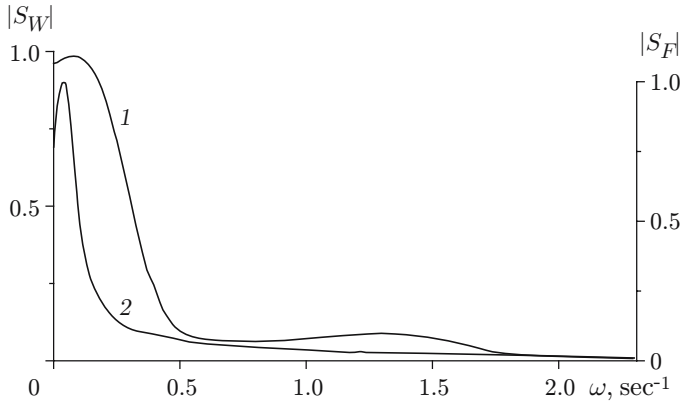

Fig. 3. Moduli of the spectra of the incident wave $|S_W|$ (curve 1) and the force $|S_F|$ (curve 2).

3. Results of Experiments. Figure 2 gives an example of synchronous variation (with time t) of the longitudinal component of the force F acting on the plate and the depth h at two points along the coordinate x. The time origin corresponds to the moment the shield emerges from water. In this example, $h_- = 0.208$ m and $h_+ = 0.125$ m. Four characteristic times t_1, t_2, t_3, and t_4 are given. At $t = t_1$, a direct wave propagated to the wavemeter located in the cross section $x = 0.985$ m. At $t = t_2$, the wave reached the wall and the force began to increase. At $t = t_3$, the reflected wave returned to the same wavemeter. We note that the wave propagation direction was not determined by a separate wavemeter; in its signal as a function of time, the leading edge of the wave was always fixed on the left. In the experiments, the direct wave in the tailwater propagated to the right, and the reflected wave to the left. The repeated increase in the depth and force at $t > t_4$ is due to the finite length of the channel not only on the right but also on the left of the shield. After reflection from the left end wall, a long seiche-type wave began to form, whose parameters depended on the channel length; in the present paper, it is not considered.

Figure 2 gives some characteristic values of the depth and force. The depth h_{as} and force F_{as} (these quantities are compared with theoretical values of h_2 and F_T) will be called asymptotic, and the depth under the first crest of the undulations $h_{\max}$ and the force $F_{\max}$ (see Fig. 2) will be called maximal.

Figure 3 gives the moduli of the oscillation spectra of the depth S_W and the force S_F normalized by their maximum values. The spectrum of S_F corresponds to curve 1 in Fig. 2, an the spectrum of S_W to curve 3. Spectral analysis was performed only in the interval of $0 \leqslant t \leqslant t_4$ (see Fig. 2) using the standard Hanning computer code. For all values of the parameter h_+^0, the maxima of the spectra were in the frequency range $0 \leqslant \omega/(2\pi) < 0.5$ sec^{-1}.

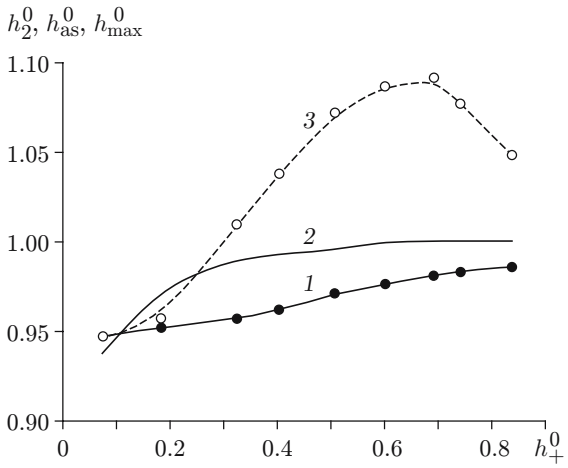

Fig. 4

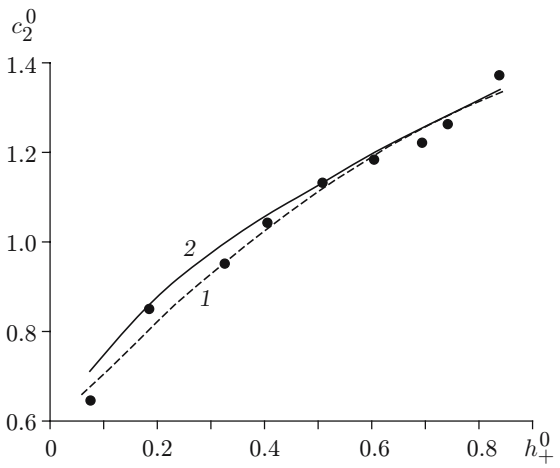

Fig. 5

Fig. 4. Characteristic values of the depth behind the reflected-wave front: h_{as}^0 (curve 1), h_2^0 calculated on basis of [1, 2] (curve 2), and $h_{\max}^0$ (curve 3).

Fig. 5. Propagation speed of the reflected wave: experiment (curve 1) and calculation based on [1, 2] (curve 2).

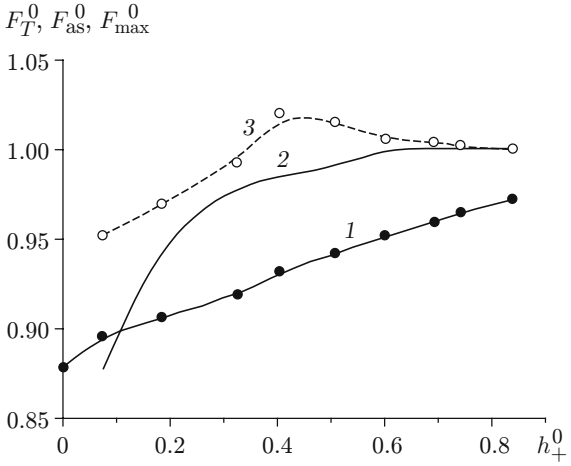

Fig. 6. Characteristic values of the force: F_{as}^0 (curve 1), F_T^0 (curve 2), and $F_{\max}^0$ (curve 3).

Curves of the theoretical depth h_2^0 and experimental depths h_{as}^0 and $h_{\max}^0$ behind the reflected wave versus the parameter h_+^0 are given in Fig. 4. The superscript 0 indicates that the depths are normalized by h_-. It should be noted that, at $h_+^0 > 0.3$, the theoretical depth behind the reflected wave differs from the initial headwater depth only slightly. The same trend is observed for the quantity h_{as}^0. In the range $h_+^0 > 0.1$, the depth h_{as}^0 is slightly smaller than the theoretical value (the difference does not exceed 2%). The depth under the first crest of the undulations can be 10% greater than the value of h_2 (at $h_+^0 \simeq 0.67$).

Figure 5 gives theoretical and experimental curves of the propagation speed of the reflected wave versus the parameter h_+^0. The speed is normalized by the quantity $c_0 = (gh_-)^{1/2}$. It is evident that the calculation results and experimental data are in good agreement. Since the depth h_{as} was slightly smaller than h_2 (see Fig. 4), the conservation condition for the discharge implies that, the experimental discharge at $x = 0$ was several percent smaller than the theoretical value.

Figure 6 gives a comparison of the theoretical, asymptotic, and maximum forces normalized by $0.5\rho g B h_-^2$. The force F_{as} can be calculated from the quantity h_{as} assuming a hydrostatic pressure distribution. This is confirmed

by independent measurements of the force (see Fig. 6), which is evidence for the reliability of the experimental data obtained. The force F_{as} is proportional to the square of the depth h_{as}; therefore, the quantities F_{as} and F_T differ to a greater extent than the quantities h_{as} and h_2. In the calculation of the force $F_{\max}$, the hydrostatic pressure distribution law is unsuitable.

Conclusions. The experiments show that the calculations for the dynamic action of a discontinuous waves on the vertical end wall of the channel based on theoretical studies [1, 2] and the experimental results differ by not more than 5%. For the impact by the incident-wave head, the maximum experimental force is greater than the calculated value, the difference being the larger for an incident wave in the form of a smooth undular bore. One method for calculating the time-varying depth on the wall after reflection of a smooth undular bore is described in [6], together with the results of an experimental verification of this method.

Similarly to the calculations based on theoretical papers [1, 2], some time after reflection of the bore head, the force becomes constant. In the range of $0 \leqslant h_+/h_- < 1/3$, the constant experimental force exceeds the theoretical value only slightly, and in the range $h_+/h_- > 1/3$, it is somewhat smaller than the theoretical value.

This work was supported by the Russian Foundation for Basic Research (Grant No. 07-01-00015) and an Integration project of the Divisions of the Russian Academy of Sciences 4.14.1.

REFERENCES

1. S. A. Khristianovich, S. G. Mikhlin, and B. B. Devison, "Unsteady motion in channels and rivers," in: *Some New Problems of Continuum Mechanics* [in Russian], Izd. Akad. Nauk SSSR (1938), pp. 15–154.
2. J. J. Stoker, *Water Waves. Mathematical Theory and Applications*, Interscience, New York (1957).
3. Chow Ven Te, *Open-Channel Hydraulics*, McGraw Hill, New York (1959).
4. A. A. Atavin, O. F. Vasil'ev, A. F. Voevodin, and S. M. Shugrin, "Numerical methods for the solution of one-dimensional problems of hydraulics," *Vod. Resursy*, No. 4, 38–47 (1983).
5. G. Colicchio, A. Colagrossi, M. Greco, and M. Landrini, "Free-surface flow after a dam-break: A comparative study," *Schiffstechnik*, **49**, No. 3, 95–104 (2002).
6. V. B. Barakhnin, T. V. Krasnoshchekova, and I. N. Potapov, "Reflection of a dam-break wave from a vertical wall. Numerical modeling and experiment," *J. Appl. Mech. Tech. Phys.*, **42**, No. 2, 269–275 (2001).
7. A. M. Frank, *Discrete Models of an Incompressible Fluid* [in Russian], Fizmatlit, Moscow (2001).
8. A. V. Gusev and V. Yu. Liapidevskii, "Turbulent bore in supercritical flow above a rough bottom," *Izv. Ross. Akad. Nauk, Mekh. Zhidk. Gaza*, No. 1, 62–70 (2005).
9. R. F. Dressler, "Comparison of theories and experiments for the hydraulic dam-break wave," *Int. Assoc. Sci. Hydrol.*, No. 38, 319–328 (1954).
10. V. I. Bukreev, A. V. Gusev, A. A. Malysheva, and I. A. Malysheva, "Experimental verification of the gas-hydraulic analogy by the example of the dam-break problem," *Izv. Ross. Akad. Nauk, Mekh. Zhidk. Gaza*, No. 5, pp. 143–152 (2004).
11. P. Scotton, "Dynamic impact of Debris flows: Experimental study," Preprint, Univ. di Trento, Trento (1996).
12. F. Trivellato and P. Scotton, "Bore impact upon a wall (experimental data base)," Preprint, Univ. Degli Studio di Trento, Trento (2001).
13. V. I. Bukreev, V. V. Degtyarev, and A. V. Chebotnikov, "Experimental technique for studying the dynamic impact of waves on obstacles," *Izv. Vyssh. Uchebn. Zaved., Sroitel'stvo*, No. 7, 70–75 (2007).
14. V. I. Bukreev and V. V. Zykov, "Bore impact on a vertical plate," *J. Appl. Mech. Tech. Phys.*, **49**, No. 6, 926–933 (2008).
15. P. G. Kiselev, *Handbook on Hydraulic Calculations* [in Russian], Gosénergoizdat, Moscow–Leningrad (1957).
16. V. I. Bukreev, "Water impingement on a vertical wall due to discontinuity decay above a drop," *J. Appl. Mech. Tech. Phys.*, **44**, No. 1, 59–63 (2003).